



PHYSICAL MODELLING AND MEASUREMENTS OF PLATE REVERBERATION

Kevin Arcas

UME-ENSTA, Chemin de la Hunière, 91761 Palaiseau, FRANCE; arcas@ensta.fr

ABSTRACT

In this article, the plate reverberation unit is studied. This effect unit has been intensively used in recording studios since the late 50's. From a mechanics point of view, this plate can be modeled by means of the Kirchhoff equations of motion of a thin linear plate. This basic model allows us to understand the common points and differences between the natural acoustic reverberation and the plate reverberation. Measurements on a EMT140 plate reverb are also presented and compared to the model predictions. The identification and modelling of the different damping mechanisms in the plate allows us to relate the reverberation time T_r to the plate physical parameters. In addition to the comprehension of the physics of the plate reverb, this work will be useful for physical modelling sound synthesis of this audio effect.

INTRODUCTION

Since the first days of broadcasting and recorded music, the artificial reverberation has been a very important tool for audio engineers. The use of close microphones to avoid noise suppresses the acoustics of the recording space. In 1926 RCA invented the reverberation chamber, the first tool to artificially replace the missing of reverberation energy. In the next 50 years, a lot of electromechanical devices were developed in order to create a reverberation effect in dry recordings [1]. One of the most acclaimed devices was the plate reverberation, in particular the EMT140 plate reverb. This unit is composed of a 2 m x 1 m size and 0.5 mm thickness flat rectangular steel plate. The plate is transversely punctually excited with an electric monophonic "dry" signal by means of an electro-dynamical actuator. The reverberated or "wet" stereophonic signal is read with two piezoelectric accelerometers that deliver an electric signal proportional to transverse punctual acceleration at two plate locations, the readout points. This unit has been extensively used by the music industry and it has become a classical effect very appreciated by audio engineers. Today, with the development of digital electronic reverberation units, using a plate reverberation in the studio has become difficult because of its fragility, bulky and expensive cost. The aim of this work is to understand the physics behind the plate reverberation in order to build a physical based sound synthesis algorithm. Physics-based sound synthesis allows very flexible means of control: the parameters which define the algorithm are directly related to the geometric and material properties of the real system.

A PLATE MODEL

The reverberation effect is produced by the plate undergoing small-amplitude vibrations. Because of the transverse excitation, the small thickness plate and the frequency range of use [20 Hz, 20 kHz], the behaviour of the plate vibrations can be modelled by the classical Kirchhoff-Love model for thin plate flexural vibrations [2]. For an isotropic material, the partial differential equation for the undamped plate is:

$$\frac{\partial^2 w}{\partial t^2} = -a^2 \nabla^4 w + f(x_{in}, y_{in}, t), \quad a^2 = \frac{Eh^2}{12\rho(1-\nu^2)} \quad (\text{Eq. 1})$$

$w(x, y, t)$ represents the transverse plate deflection, and a^2 is the stiffness parameter. (Eq.1) is defined over the region $x_{in} \in [0, L_x]$, $y_{in} \in [0, L_y]$. ∇^4 is the biharmonic operator. E , h , ρ and ν are Young's modulus, plate thickness, density and Poisson's ratio, respectively for the plate. $f(x_{in}, y_{in}, t)$ represents the input waveform source located at the driving point (x_{in}, y_{in}) .

Under harmonic excitation, we can derive the dispersion relation of the medium. This links the wavenumber γ and the angular frequency ω , and is: $\omega^2 = a^2 \gamma^4$.

WAVE PROPAGATION

In natural reverberation, the propagation of acoustic waves in the air is non-dispersive at velocity c_a . Because of this non-dispersive propagation, there is no distortion in wave propagation in acoustic spaces. This allows to easily identify the direct sound and the echoes at the beginning of the impulse response. In the case of plates, the phase velocity c_{ph} and the group velocity c_{gr} can be easily derived from the dispersion relation and are:

$$c_{ph} = \frac{\omega}{\gamma} = \sqrt{a\omega} \quad c_{gr} = \left(\frac{d\omega}{d\gamma} \right)_{\gamma_0} = 2\sqrt{a\omega} \quad (\text{Eq. 2})$$

At a given frequency, the phase velocity defines the spatial distribution of the wave into the medium (the wavenumber). The group velocity is related to the vibration energy propagation. Both velocities are proportional to the frequency root square: the medium is dispersive and high frequencies travel faster than low frequencies. Because of the dispersion of flexural waves, the input signal is distorted and it is not possible to find the same waveform at the readout points of the plate for the direct sound and the early reflections. This is one of the main differences between natural reverberation and plate reverberation.

The simple form of group velocity allows us to experimentally identify the stiffness parameter a^2 from (Eq. 1). This parameter can not be known from tables because of the physical properties variability between different steel varieties. Tone burst excitation, with energy content centered at a frequency f_0 , is used for exciting the plate with a shaker. Time domain accelerations are measured by three accelerometers aligned along the horizontal x axis. The reference accelerometer is located at the center of the plate and the other two at 30 cm and 60 cm from the reference on its right-hand side. Since the signal is dispersive, it is not trivial to find the group velocity from two acceleration measurements (the reference and another one). A technique inspired by seismic signal processing has been developed to estimate the propagation time of the energy between two accelerometers. The time propagation of the wave packet is computed as the first maximum of the envelope of the two signals intercorrelation. The envelope is computed as the magnitude of the analytical signal, which is computed with the signal Hilbert Transform [3]. Fig.1 shows the acquisition for the experiment at $f_0 = 3000 \text{ Hz}$ and the signal processing estimation of the wave packet travelling time. The choice of the tone burst length should be sufficiently short to avoid reflection interferences on the measurements. These measurements have been carried out for several frequencies between 500 Hz and 15 kHz . Fig.2 shows the group velocity results for the different measurements and the c_{gr} curve obtained from the least squares fit of c_{gr}^2 (Eq.2) to the measurements from both accelerometers. The good agreement obtained in the group velocity frequency behaviour confirms the value obtained for the stiffness parameter $a = 0.7846$.

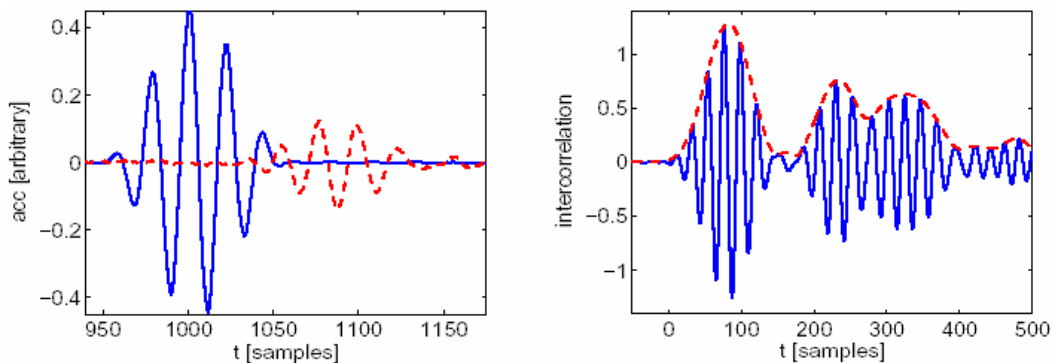


Figure 1.- Left: temporal signals of the reference accelerometer and at 30 cm from it. Right: Intercorrelation and its envelope which maximum gives the propagation time of the wave packet. Parameters: 5-period tone burst at $f_0 = 3000 \text{ Hz}$, sampling frequency $F_s = 65536 \text{ Hz}$.

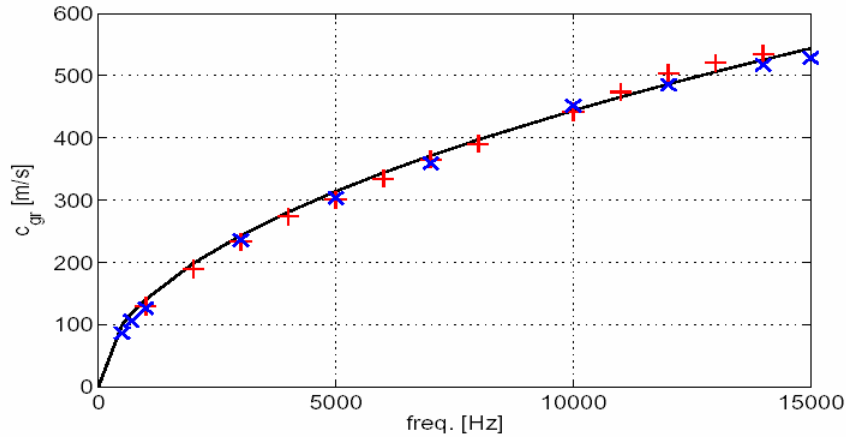


Figure 2.- Group velocity function of the frequency. Experimental: 'x' accelerometer at 30 cm and '+' accelerometer at 60 cm. The continuous curve is the fitted theoretical value of c_{gr} from (Eq. 2) with $a = 0.7846$.

Since the energy propagation in the plate is determined by the a value, we can estimate direct-path time delay for each readout point, which depends on frequency. In the audible range [20 Hz, 20 kHz], the group velocity is between 20 m/s and 628 m/s. The EMT140 left and right readout points are located at a distance of 0.6 m and 0.88 m from the driving point respectively. The frequency dependent time delay of energy arrival is between 30.3 ms and 1.0 ms and between 44.3 ms and 1.4 ms respectively. The human hearing system can perceive this delay [4]. The well-known psychoacoustics precedence effect can have an important role in plate reverberation because of the early arrival of high frequency energy.

FREQUENCY STATISTICS

Since the first works on artificial reverberation, two realism criterions have been identified as very important for the perception of the late reverberation: the echo density and the modal density [5]. For the first one, it is accepted the need of at least 10000 echos / s [6], but we have seen that there are no echoes in the plate reverb: the input signal is spread because of the dispersive propagation. In the frequency domain, the modal density represents the number of modes that can be found by Hertz. We can compare the modal density behaviour of a room with the plate's one. The modal density of a rectangular room with rigid boundaries is given by [7]:

$$D_m(f)_r = \frac{\partial N_m(f)}{\partial f} \approx 4\pi L_x L_y L_z \frac{f^2}{c_a^3} \quad (\text{Eq. 3})$$

$D_m(f)_r$ is proportional to the square of the frequency. For a plate, the modal density asymptotic value is independent of boundary conditions and it can be computed from the simply supported plate configuration. In this simple case, we have analytical expressions for the modal frequencies of the plate, and the mode count $N_m(f)$ can be easily performed. The modal density is [8]:

$$D_m(f)_p = \frac{\partial N_m(f)}{\partial f} \approx \frac{L_x L_y}{2a} - (L_x + L_y) \sqrt{\frac{1}{8\pi a f}} \quad (\text{Eq. 4})$$

When frequency grows, the second term of $D_m(f)_p$ vanishes and the modal density of the plate is almost constant. Its value depends only on the plate area $L_x L_y$ and the stiffness parameter a . This justifies the big area and small thickness of the EMT140 plate reverberation, for which the numerical application of (Eq.4) gives $D_m(f)_p = 1.27 \text{ modes/Hz}$. For artificial reverberation design, Schroeder preconises a minimum value for $D_m(f)$ equal to a quarter of the reverberation time T_r [5]. The EMT140 unit verifies this constraint for T_r lower than 5.1s.

In order to verify the validity of the $D_m(f)_p$ calculus the experimental measurement of $D_m(f)_p$ has been done on the reverberation plate. Modal density accurate measurement techniques are well-known because its values are very important in order to use Statistical Energy

Analysis(SEA) with a higher order of confidence. According to Clarkson [9], the modal density could be obtained from the real part of the driving point admittance using the relation:

$$D_m(f)_p = 4MRe(Y) \quad (\text{Eq. 5})$$

Where M is the mass of the structure (steel density $\rho = 7860\text{Kg/m}^3$), and $Re(Y)$ is the real part of the driving point admittance. For the measurement of Y we use a 4810 B&K shaker with a B&K 8001 impedance head. Mass correction must be considered when making mobility measurements on a lightweight structure because added masses from the admittance head and attachment values will corrupt the force measurement. For high frequencies measurement, the more reliable technique is to use the dynamic mass of the shaker $H_{ma} = a(\omega)/F(\omega)$ to correct the measured admittance Y_m .

$$Y_a = \frac{Y_m}{1 - (Y_m/Y_M)} = \frac{Y_m}{1 - (j\omega Y_m/H_{ma})} \quad (\text{Eq. 6})$$

H_{ma} is obtained by measuring the point mobility of the added mass attached to the impedance head when separate from the structure. The experimental frequency dependent modal density versus the theoretical value are presented in Fig.3. The very good agreement between both values confirms our approach.

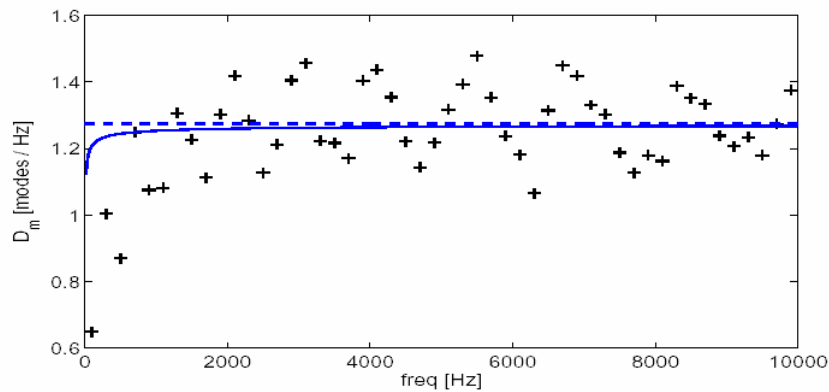


Figure 3.- Modal density for the EMT140 plate reverb. Experimental results in 200 Hz frequency bands(+). The solid line is the theoretical value computed with (Eq.4) and the dashed line is its asymptotic value.

DAMPING MECHANISMS

Since reverberation time T_r is the most accepted objective measure of reverberation it is important to understand the damping properties in metallic plates. Lambourg's works on metallic plates sound synthesis conclude that the two most important damping mechanisms for these plates are thermoelastic and radiation damping [10]. In the EMT140 plate reverb there is also a damping control induced by a porous plate parallel to the steel plate. Damping in the low-mid frequency range increases when the porous plate is approached. The distance d between both plates can be manually set between 11 mm and 66 mm.

Damping measurements

The decay behaviour of plate vibrations has the general form $\exp(-at)$, where the damping factor a depends on the frequency. The damping factor a of the EMT140 is estimated from the impulse response (IR) of the plate at progressive distance d of the porous plate configurations. The EMT140 original driver is used for excitation and an accelerometer is placed beside the EMT140 right readout point. IR measurements are done with 100 seconds log-sweep excitation signals in the audible frequency range. The IR is synthesised by convolving the obtained response with the inverse filter of the excitation signal (see [11] for details). For each frequency band, the mean damping factor is computed by means of the Schroeder Energy Decay Curve [12] of each frequency band of the IR's short time fourier transform (4096 FFT points and 90 % overlapped). Experimental damping factors are presented in Fig.4.

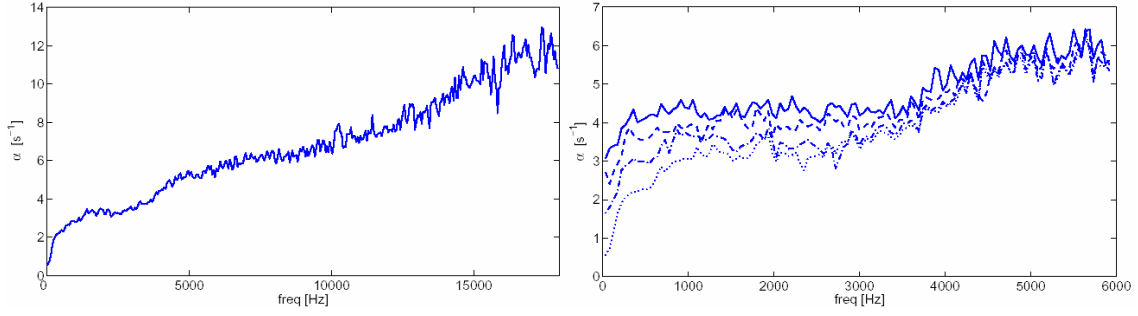


Figure 4.- Right: damping factor measurements for the porous plate as far as possible: $d=66\text{mm}$.
Left: Damping factor measurements for progressive d values: (11.0, 13.2, 17.3, 66) mm.

Thermoelastic damping

Thermoelastic damping is induced by the coupling between thermal waves and strain waves. This is the main intrinsic damping mechanism present on metallic plates at low frequencies [10]. This damping is more important for flexural modes than for torsional modes. For a plate flexural mode, an approximation of the thermoelastic damping factor $\alpha_{th}(\omega)$ is:

$$\alpha_{th}(\omega) = \frac{\omega^2 R_1 C_1}{2((C_1/h)^2 + h^2 \omega^2)} \quad \alpha_{th} |_{\omega \rightarrow \infty} = \frac{R_1 C_1}{2h^2} \quad (\text{Eq. 7})$$

R_1 and S_1 are only dependent on material elastic and thermal properties. For a given material, this damping is proportional to the inverse square of the plate thickness. For the EMT140 steel plate, the numerical application of (Eq.7) gives:

$$R_1 = 4.94 \cdot 10^{-3}; \quad C_1 = 2.98 \cdot 10^{-4}; \quad \alpha_{th\infty} = 2.95\text{s}^{-1} \quad (\text{Eq. 8})$$

This analysis allows us to compute the $\alpha_{th\infty}$ for the same plate thickness and other plate materials such as gold, copper or aluminium: the $\alpha_{th\infty}$ values are 5.9 s^{-1} , 7.39 s^{-1} and 10.8 s^{-1} . We conclude that the interest of using steel in the EMT140 plate reverb is its small amount of thermoelastic damping compared to other metals. This allows for longer T_r values at low frequencies. Left Fig.5 presents the damping predicted by the thermoelastic model.

Finite Plate radiation damping

Radiation damping is produced by the transformation of vibration energy into acoustic energy. Below the critical frequency $f_c = c_a^2 / 2\pi a$, sound is radiated less efficiently and there is less radiation damping of vibrations. As for the modal density analysis, we see the interest of having a small stiffness parameter: for the EMT140 plate we find $f_c \approx 25\text{ kHz}$. Maidanik developed an averaged radiation efficiency σ expression for a simply supported baffled plate for frequencies $f < f_c$. Because of the high modal density, we can approach our plate by Maidanik expression [13] and neglect the corner modes contribution which is very small compared to the edge modes contribution. We can derive the damping factor α_{rad} from σ and obtain

$$\alpha_{rad} = \frac{1}{2\pi^2} \frac{c_a \rho_a}{\rho h} \frac{L_x + L_y}{L_x L_y} \frac{c_a}{f_c} g \quad \text{where: } \psi = \sqrt{\frac{f}{f_c}}$$

$$g = \frac{(1 - \psi^2) \ln[(1 + \psi)/(1 - \psi)] + 2\psi}{(1 - \psi^2)^{3/2}}; \quad (\text{Eq. 9})$$

The behaviour of this radiation losses model for the EMT140 plate is presented in the left Fig.5.

Porous plate radiation damping

Modelling the radiation increase of a vibrating plate with a parallel porous plate at a distance d has been already studied by Cummings [14]. He approached the problem with an infinite plate approximation to obtain an analytical expression of the radiation efficiency increase. The porous

material is characterised by its flow resistivity and its porosity. The radiation damping increase can be directly derived from the radiation efficiency increase. Right Fig.5 presents the EMT140 damping increase predicted by this model. The comparison with our measurements resulted in a very good agreement for $f > 200$ Hz. At lower frequencies the model underestimates the radiation increase and the infinite plate approximation is not valid. This can be certainly improved by means of modal analysis [14].

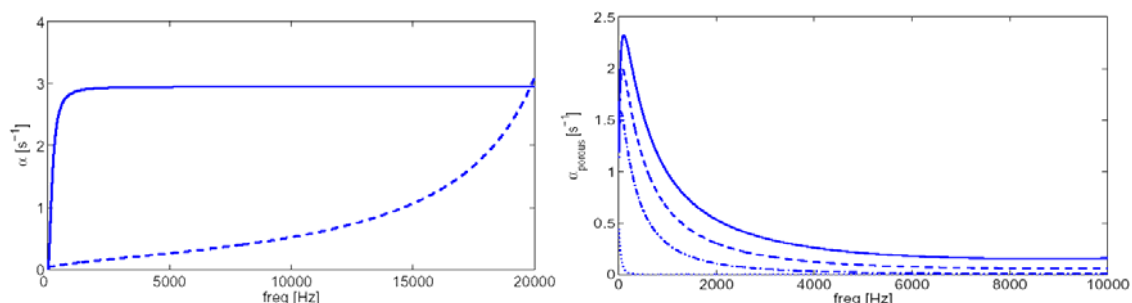


Figure 5.- Left: EMT140 thermoelastic (continuous) and radiation (dashed) damping factors predicted by the models. Right: damping factor added by the porous plate estimated by the Cummings model for different distances between both plates, $d = (65.8, 17.3, 13.2, 11.0)$ mm.

CONCLUSIONS

Measurement and a physical model of the plate reverberation unit have been performed. These works will contribute to improve our finite differences plate reverberation sound synthesis. However, the very low frequency damping due to the porous plate is not completely understood. In order to validate our model, experimental study of the gold foil reverb EMT240, will be performed soon. The EMT240 has an $18 \mu\text{m}$ thickness and $270 \text{ mm} \times 290 \text{ mm}$ size gold plate. We expect these measurements to be in accord with our model. Other future research directions concern the development of a real time sound synthesis based on the physical model. Last, but not least, several impulse response measures and sound synthesis are available at the author's website <http://wwwy.ensta.fr/~arcas>.

References

- [1] B. Blesser. An interdisciplinary synthesis of reverberation viewpoints. J. Audio Eng. Soc., 49(10):867-903, October 2001
- [2] K. Graff. Wave Motion in Elastic Solids. Dover, New York, USA, 1975
- [3] A. V. Oppenheim and R. W. Schaffer. Discrete-Time Signal Processing. Prentice Hall, Inc., 1989
- [4] J. Blauert. Spatial Hearing. M.I.T. Press, 1997
- [5] M. R. Schroeder. Natural sounding artificial reverberation. J. Audio. Eng. Soc., 10(3):219-223, 1962
- [6] D. Griessinger. Practical processors and programs for digital reverberation. Proc. 7th AES Int. Conf., pp 187-195, 1989
- [7] H. Kuttruff. Room Acoustics. Applied Science Publishers, London, 2nd edition, 1979
- [8] G. Xie, D. J. Thompson and C. J. C. Jones. Mode count and modal density of structural systems: relationships with boundary conditions. Journal of Sound and Vibration, 274:621-651, 2004
- [9] B. L. Clarkson. The derivation of modal densities from point impedances. Journal of Sound and Vibration, 77:583-584, 1981
- [10] A. Chaigne and C. Lambourg. Time-domain simulation of damped impacted plates. part i. theory and experiments. J. Acoust. Soc. Am., 190(4):1422-1432, 2001
- [11] A. Farina. Simultaneous measurement of impulse response and distortion with a swept-sine technique. 108th AES Convention, 2000
- [12] M. R. Schroeder. New method for measuring reverberation time. J. Acoust. Soc. Am., 37:409-412, 1965
- [13] G. Maidanik. Response of ribbed panels to reverberant acoustics fields. J. Acoust. Soc. Am., 34:809-826, 1962
- [14] A. Cummings Sound radiation from a plate into a porous medium. Journal of Sound and Vibration, 247(3):389-406, 2001